Behavioral/Systems/Cognitive

Impaired Auditory Temporal Selectivity in the Inferior Colliculus of Aged Mongolian Gerbils

Leila Khouri,[1,3] **Nicholas A. Lesica,**[2] **and Benedikt Grothe**[1,3]

[1]Division of Neurobiology, Department Biology II, Ludwig Maximilians University of Munich, 82152 Martinsried, Germany, [2]Ear Institute, University College London, London, WC1X 8EE, United Kingdom, and [3]Integriertes Forschungs- und Behandlungszentrum für Schwindel, Gleichgewichts- und Okulomotorikstörungen, 81377 Munich, Germany

Aged humans show severe difficulties in temporal auditory processing tasks (e.g., speech recognition in noise, low-frequency sound localization, gap detection). A degradation of auditory function with age is also evident in experimental animals. To investigate age-related changes in temporal processing, we compared extracellular responses to temporally variable pulse trains and human speech in the inferior colliculus of young adult (3 month) and aged (3 years) Mongolian gerbils. We observed a significant decrease of selectivity to the pulse trains in neuronal responses from aged animals. This decrease in selectivity led, on the population level, to an increase in signal correlations and therefore a decrease in heterogeneity of temporal receptive fields and a decreased efficiency in encoding of speech signals. A decrease in selectivity to temporal modulations is consistent with a downregulation of the inhibitory transmitter system in aged animals. These alterations in temporal processing could underlie declines in the aging auditory system, which are unrelated to peripheral hearing loss. These declines cannot be compensated by traditional hearing aids (that rely on amplification of sound) but may rather require pharmacological treatment.

Introduction

Studies on speech recognition report detrimental effects of adverse listening conditions on performance of aged humans (Gustafsson and Arlinger, 1994). Because information in speech is conveyed primarily by temporal fluctuations of signal amplitude, it has been assumed that the decline in speech recognition in noise is caused by alterations in temporal processing (Gordon-Salant and Fitzgibbons, 1993). Accordingly, the duration of the minimal detectable gap in noise is increased for aged humans and experimental animals (Snell, 1997; Strouse et al., 1998; Barsz et al., 2002; Hamann et al., 2004).

There is mounting evidence that auditory temporal processing relies on a balanced and timed interplay of excitation and inhibition (Grothe, 1994; Grothe et al., 2001; Brand et al., 2002; Pecka et al., 2008). In aged animals, presynaptic and postsynaptic levels of the inhibitory neurotransmitters glycine and GABA and their respective receptors are significantly reduced (Banay-Schwartz et al., 1989; Milbrandt et al., 1994, 1996, 1997, 2000; Willott et al., 1997; Krenning et al., 1998; Burianova et al., 2009), potentially disrupting the balance of excitation and inhibition.

In the auditory midbrain, the inferior colliculus (IC) receives inputs from excitatory and inhibitory projections from virtually all other auditory nuclei (Oliver and Huerta, 1992; Casseday et al., 2002). A variety of response properties are created in the IC that critically depend on inhibition (Irvine and Gago, 1990; Faingold et al., 1991; Fuzessery and Hall, 1996; Ehrlich et al., 1997; LeBeau et al., 2001; Pollak et al., 2003a,b), for example, selectivity to frequency modulations (Woolley and Casseday, 2005; Andoni et al., 2007), amplitude modulations (AMs) (Langner and Schreiner, 1988; Krishna and Semple, 2000; Joris et al., 2004), and duration (Casseday et al., 1994; Brand et al., 2000; Pérez-Gonzáles et al., 2006). In accordance with decreased synaptic weight of inhibitory inputs, studies on IC responses in aged rats (Shaddock Palombi et al., 2001) and mice (Walton et al., 2002) report altered tuning to AM parameters.

An important consequence of the response selectivity of IC neurons is heterogeneity of receptive fields of the IC neuron population. Heterogeneous receptive fields can increase the information encoded in population activity (Shamir and Sompolinsky, 2006; Chelaru and Dragoi, 2008). A recent study in the IC reports that heterogeneity of neuronal responses lead, relative to lower auditory nuclei, to a decrease in signal correlations over the IC population, which could increase the encoding efficiency for natural stimuli (Holmstrom et al., 2010).

We hypothesized that a loss of inhibition would reduce the selectivity and consequently the heterogeneity of IC responses and the efficiency of encoding in populations of IC neurons. We used synthetic amplitude modulated stimuli to assess selectivity and diversity of tuning to temporal modulations, and we used natural stimuli to assess efficiency of coding. We show that neurons from aged animals are less selective for temporal modulations, temporal receptive fields are consequently less heterogeneous, and population encoding is more effective for neurons from young adult than for neurons from aged animals.
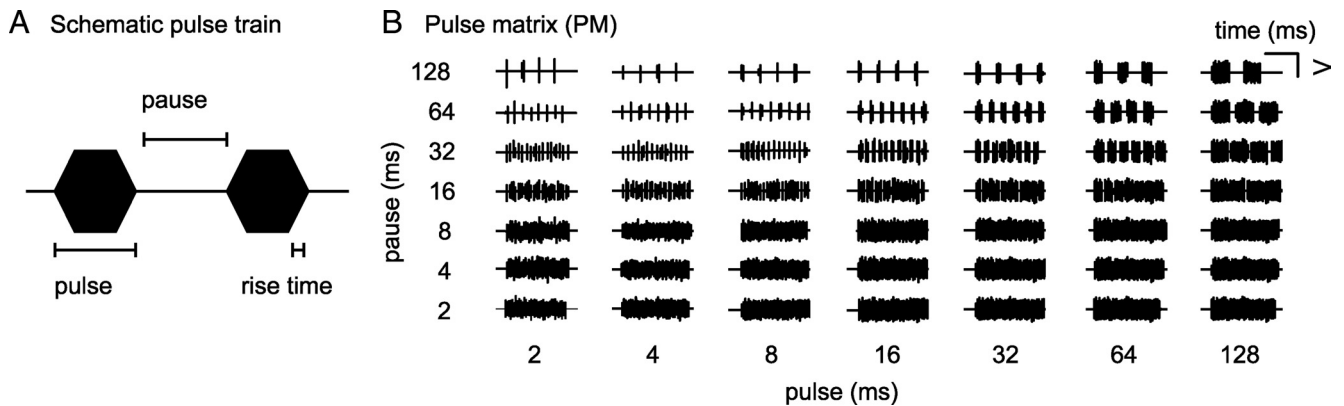
Figure 1. Pulse matrix. ***A***, Schematic of a pulse train consisting of two trapezoid pulses with 1 ms rise and fall times each. Pulse duration is defined as the entire duration of the pulse including rise and fall time; pause duration is defined as the entire silent interval between pulses. ***B***, Pulse matrix. The pulse matrix consists of 49 trains of trapezoid broadband noise pulses. Pulse and pause duration span from 2 to 128 ms in logarithmic intervals. Pulse trains are 512– 640 ms long.

Materials and Methods

Action potentials in response to auditory stimuli were recorded *in vivo* from single IC neurons of 15 young adult (3 ± 1 months) and 11 aged (39 ± 4 months) Mongolian gerbils (*Meriones unguiculatus*) of both sexes. All experiments were approved according to the German Tierschutzgesetz (55.2-1-54-2531-57-05 Regierung Oberbayern).

Surgical procedures. The surgical procedures applied in this study were described in detail previously (Siveke et al., 2006) and were essentially the same for young adult and aged gerbils. Briefly, gerbils were anesthetized by an initial intraperitoneal injection (0.5 ml/100 g body weight) of a physiological NaCl solution (Ringer's solution) containing ketamine in 20% v/v and xylazine in 2% v/v concentration. During surgery, a dose of 0.05 ml of the ketamine/xylazine mixture was applied subcutaneously every 30 min. During recording, animals were injected continuously with anesthesia via an automatic pump (801 Syringe Pump; Univentor) at a pump rate of 1.7–3 μl/min, depending on body weight. Animal body temperature was monitored and, if necessary, adjusted using a thermostatically controlled heating pad. Before recording, skin and tissue covering the upper part of the skull were removed carefully. A small metal rod was mounted on the frontal part of the skull to secure the head of the animal in a stereotaxic device during recordings.

After surgery, the animal was transferred into a sound-attenuated chamber, and the animal's head was fixed in a custom-made stereotaxic device (Schuller et al., 1986). A craniotomy and a durotomy were performed at 1.3–2.6 mm lateral to the midline and 0.5–1 mm caudal to the bregmoid axis. After recording, the animal was killed by injection of 1 ml of 20 mg/ml pentobarbital in Ringer's solution. The position of the electrode was marked by a lesion induced by a sinusoidal current of 20 kHz and 10 μA for 90 s. The brain was removed from the head and was fixed in 4% paraformaldehyde for 2 d. The brain was then transferred to 30% sucrose and was stored at 4°C for 2 d. Subsequently, the brain was placed in tissue medium, frozen solid, and cut in a standard plane for sections. Transverse 45 μm sections were cut in a cryostat at −21°C. The sections were then Nissl stained, and recording sites were verified via light microscopy.

Neural recordings. Tungsten electrodes, of 3–7 MΩ impedance, were mounted in a seven-electrode system (Thomas Recordings). A custommade glass tube with an inner diameter of ~300 μm at the tip was attached to the shaft probe of the multielectrode to reduce the interelectrode distances to ~80–300 μm. After craniotomy and durotomy, the multielectrode array was introduced in the brain at a 90° angle to the brain surface (bregma–lambda plane), and electrodes were advanced to the central IC, starting ~2 mm below the brain surface. Electrodes were moved individually to isolate single-unit signals. Action potentials were conventionally amplified, converted to digital signals [RX5; Tucker Davis Technologies (TDT) System 3], and fed to a computer running Brainware (Jan Schnupp, University of Oxford, Oxford, UK, for TDT System 3). For each cell, spike waveforms were identified initially during the experiment and were verified carefully offline by spike-sorting analysis (MClust, Free-ware spike sorting by David Redish,

University of Minnesota, Minneapolis, MN; available at redishlab. neuroscience.umn.edu/MClust/MClust.html).

Acoustic stimulation and recording protocol. Acoustic stimuli were built in Matlab, converted to analog signals (DA3-2/RP-2; TDT), and delivered to loudspeakers (ER-2; Etymotic Research) by TDT System 3 hardware. The output of the loudspeakers was guided to the ear canal in a sealed system. Frequency response and energy in frequency bands were verified using calibrated probe tube microphones (ER10B+; Etymotic Research). The sound signal was amplified and transferred to the computer for analysis before the recording. The input to the electrostatic speakers was corrected to create an output of constant amplitude from 500 Hz to 12 kHz. [Although gerbils' audible frequencies range up to 50 kHz (Ryan, 1976), we chose speakers with a frequency range up to 12 kHz. This range of frequencies covers the range of frequencies present in our stimuli.]

Animals were presented with monaural white-noise bursts of 100 ms duration with 5 ms linear rise and fall times at repetition rates of 4 Hz, while electrodes were advanced through the IC contralateral to the site of stimulation. When a single unit was encountered, stimulation was switched to pure tone stimuli of 100 ms duration (rise–fall time adjusted to avoid spectral artifacts) at various frequencies and sound pressure levels. From the acquired frequency response areas, best frequency (BF) (frequency to which the neuron was most sensitive), threshold (lowest sound pressure level to elicit neuronal discharge or to suppress spontaneous activity), and temporal response types (described in Results) were determined. Neurons were clustered into temporal response type classes based on the temporal pattern of their response to a pure tone at BF 20 dB above threshold.

Ninety-five aged and 92 young adult neurons were presented with 49 sequences of broadband noise bursts gated with symmetrical trapezoid functions of, within sequences, constant width and repetition rate. Although sinusoidal amplitude modulated stimuli (SAM) are commonly used to analyze neuronal temporal processing, we chose to infer indicators for temporal selectivity from rate responses to a matrix of noise burst sequences [pulse matrix (PM)]. The reason is that IC neurons are not exclusively sensitive to modulation frequency but are also sensitive to pulse duration, pause duration, and rise time of the stimulus (Krebs et al., 2008). These parameters cannot be independently varied using SAM stimuli. In our PM, we varied the duration of noise pulses and the duration of silent intervals between pulses (pause) in seven logarithmic steps from 2 to 128 ms. Thus, a matrix of 49 stimuli of different combinations of pause and pulse duration was created (Fig. 1*B*). Rise and fall times of trapezoidal noise pulses lasted 1 ms each (Fig. 1*A*). The PM was presented to the animal at 20 dB above noise threshold.

To classify neurons in relation to their response pattern to PM stimuli, cells were stimulated with nine repetitions of 250 ms trapezoid broadband noise bursts (frozen) at 20 dB above noise threshold and sorted according to their temporal response pattern (described

Table 1. Temporal response patterns: classification scheme

	Response components		
Temporal response pattern	Onset (first 50 ms of stimulation)	Ongoing (remaining stimulation time)[a]	Offset (from stimulation offset)[b]
Sparse (spa)	<2 Hz	<2 Hz	≤Mean (on, ongoing)
Onset (on)	>2.5 Hz	<1.5 Hz	Not specified[c]
Primary-like (pl)	>1.5× ongoing	>1.5 Hz	0 Hz
Sustained (sus)	>2 Hz and ≥1.5× ongoing	>2 Hz and ≤2× onset	0 Hz
Primary-like spontaneous (plb)	1.5× ongoing	>1.5 Hz and >offset + SD (offset)	>0 Hz
Sustained spontaneous (sub)	>2 Hz and ≥1.5× ongoing	>2 Hz and ≤2× onset	>0 Hz
Long-latency sustained/build-up (lsus)	Not specified	>2× onset	Not specified[c]
Offset/inhibitory (off)	<offset − SD (offset) or no activity	<offset − SD (offset) or no activity	>0 Hz

[a]Remaining stimulus time, 60–110 ms for pure tone stimulation and 60–260 ms for noise stimulation.

[b]From stimulus offset, Activity from 120 to 250 ms from stimulus onset for pure tone (pulse duration, 100 ms) and 270 to 750 ms for noise (pulse duration, 250 ms) stimulation.

[c]Onset and late sustained neurons were not subdivided in spontaneously not active and active cells because only 2 of 7 onset cells and 2 of 5 late sustained cells in young and 1 of 5 onset cells and 5 of 10 late sustained neurons in aged animals showed spontaneous activity.

below and in Results) offline. Repetition rate of noise pulses was 1.3 per s.

Fifty-seven young adult and 47 aged IC neurons were additionally stimulated with eight speech snippets taken from a clinical test (Oldenburger Satztest, sample sentences kindly provided by Dr. Birger Kollmeier, Universitaet Oldenburg, Oldenburg, Germany) at 20 dB above noise threshold. From these recordings, the first 125 ms were used for analysis. This time window corresponds to the first one to two letters from each of the eight snippets (specifically, Br, Ta, St, Ni, K, Pe, Ul, Do).

Presentation order of stimuli was randomized (interleaved). We recorded responses to at least nine repetitions of each stimulus.

Temporal response types. Response type classes [sparse, onset, primary like, sustained, late sustained (including long-latency sustained and build-up neurons), and offset (including offset and inhibitory neurons); described in Results (Table 1, Fig. 2)] were identified from responses to 10 repetitions of pure tones at best frequency and to 9 repetitions of 250 ms frozen noise bursts. Classification was performed using a Matlab routine dependent on the onset component (first 50 ms), the ongoing component of the response (50 ms for tones and 200 ms for noise), and activity after sound offset (20 ms after sound offset to 150 ms after sound offset for tones and 20–500 ms after sound offset for noise). For poststimulus time histograms (PSTHs), spikes were binned in 5 ms bins.

We used the Matlab built-in bootstrapping ("bootstrp") routine to obtain significance values for differences we observed between distributions of temporal response patterns of neurons from young adult and aged animals. This routine drew 5000 subsamples from our actual samples of neurons. From the distribution of subsamples of neurons from young adult animals we obtained from bootstrp, we calculated the probability to obtain the observed value from the aged distribution for each temporal response type.

PM receptive fields. PM receptive fields are defined as the relation between the temporal frequency of action potentials evoked between 10 and 510 ms of stimulus presentation, and pulse and pause duration of the stimulus pulse train.

Temporal selectivity index. An index of temporal selectivity (TSI) was calculated from PM receptive fields as follows:
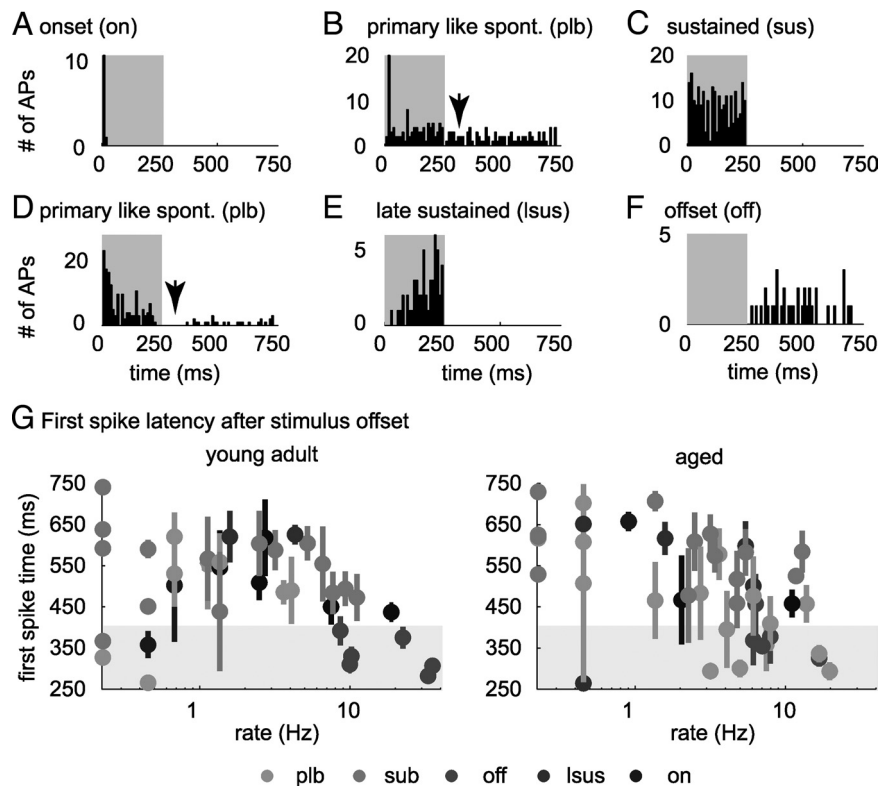

Figure 2. Types of neuronal response patterns evoked by broadband noise. *A–F* show PSTHs (bin width, 5 ms) of selected neurons from six temporal response types in response to 250 ms broadband noise pulses. Gray shaded areas indicate the duration of the stimulus. All neurons were recorded from aged animals. *A*, Onset (on) neuron, discharging during the first 50 ms of stimulus presentation. *B*, Spontaneously (spont.) active primary-like neuron (plb), responding ≥30% stronger during stimulus onset (first 50 ms) than during the later portion of the stimulus. Note that this neuron (in contrast to the neuron presented in *D*) does not show a dip in discharge after stimulus offset (arrows in *B* and *D*). This behavior was exclusively observed for aged neurons. *C*, Sustained neuron (sus). This type of neuron showed a sustained discharge pattern during the entire sound presentation. *D*, Spontaneously active primary-like neuron (plb), which discharged with a primary-like pattern during sound presentation, paused, and recovered spontaneous activity during the silent interval between noise burst presentations. *E*, Late sustained/build-up neuron (lsus). This type of neuron exhibited a build-up or a sustained discharged pattern after a latency of ≥50 ms. *F*, Offset/inhibitory neuron (off); neurons from this class either suppressed discharge below spontaneous activity during stimulus presentation or exclusively discharged after stimulus presentation. *G*, Absolute time of first action potential after stimulus offset (mean ± SD over repetitions) versus rate of discharge between stimuli for spontaneously active neurons. Response types of neurons are coded in colors: onset (on), primary-like (plb), sustained (sub), late sustained (lsus), offset (off), and sparse (spa) cells that showed spontaneous activity. Whereas in young adult animals, only offset neurons strongly discharged within 150 ms after stimulus offset, in aged animals, primary-like and offset neurons strongly discharged within 150 ms in aged animals (gray shaded areas).

$$TSI = \frac{max(rPM) - min(rPM)}{max(rPM)}, \quad (1)$$

where rPM stands for discharge rate evoked by PM. The index assumes a value of 1, if the cells discharge rate is modulated to 0 in response to any

pulse train in our PM (and the neurons response is therefore highly selective), and assumes a value of 0, if the cells discharge rate is constant over the PM space (and the neurons response is therefore unselective).

Pearson's correlation coefficient. As a measure of similarity, Pearson's correlation coefficients (r) were calculated between PM receptive fields of every possible pair of cells:

$$r(i,j) = \frac{E((x_i - Ex_i) \times (x_j - Ex_j))}{\sqrt{E((x_i - Ex_i) \times (x_i - Ex_i)) \times E((x_j - Ex_j) \times (x_j - Ex_j))}},$$
(2)

where E signifies the expected value or mean, and x_i and x_j signify cell 1 and cell 2 in a pair of cells.

Principal component analysis. Principal components (PCs) and eigenvalues of the covariance matrix (the variance explained) were computed based on PM receptive fields of single neurons. Mean of PM receptive fields was subtracted before analysis. To compare influence of PCs on individual PM receptive fields, distributions of weights (the coordinates for the representation of each individual PM receptive field in PC space) was analyzed first separately for PCs 1–3. Second, to illustrate the change in shape of PM receptive fields between young adult and aged animals, neurons were clustered based on their coordinates in three-dimensional PC space, using the Matlab built-in "kmeans" clustering algorithm. The algorithm yielded robust clusters using Euclidean distances: for each neuron, the mean distance to neurons within its assigned cluster was much smaller than the distances to neurons assigned to different clusters. Separation of cluster centroids was tested using a multivariant ANOVA (MANOVA).

Spike distance metric. Trains of action potentials in response to human speech were analyzed in terms of dissimilarity. To achieve this, we used a decoding paradigm. To decode a response evoked by one trial of one sentence from our set, we removed it from the set and used a distance metric to infer the stimulus that evoked it. The metric enables us to compute the average distance from the response we picked, to all of the responses evoked by a given stimulus, except itself. We then chose the stimulus for which the average distance to the response was minimal. Instances of correct classification of responses to a certain stimulus were counted and divided by the number of stimulus presentations to obtain classification success.

Different metrics have been proposed to compute the distance between responses (Victor and Purpura, 1996; van Rossum, 2001). We calculated distances between responses based on spike counts using the metric proposed by Victor and Purpura (1996) (software available at http://neuroanalysis.org/toolkit). Details of the implementation of the metric have been described previously by Victor and Purpura (1996) and Aronov (2003). To decode speech snippets from populations of neurons, we calculated distances for each cell separately and then summed distances over cells before decoding.

To quantify heterogeneity of encoding patterns, we computed (1) for each neuron the percentage correct classifications achieved when decoding the set of eight speech snippets from the single neuron responses, and (2) for every possible pair of neurons (within each population), the percentage correct classifications achieved when decoding the set of eight speech snippets from the responses of the pair of neurons. We then measured the increase in percentage correct classification of speech snippets (difference in percentage correct classification of speech snippets, in case classification was based on responses from one neuron and in case classification was based on responses from two neurons) that paired encoding caused for each neuron.

Results

To compare the neural representation of the temporal parameters of the auditory stimulus, we recorded extracellular action potentials from 133 neurons located in the central nucleus of the IC of 15 young adult (3 ± 1 months) and 112 IC neurons from 11 aged (39 ± 4 months) Mongolian gerbils. Before we analyzed how these cells encoded temporal stimulus parameters (amplitude modulations), we characterized and compared neurons

from young adult and aged animals in terms of BF, single-neuron thresholds, temporal discharge patterns evoked by acoustic stimulation with pure tones and broadband noise, and spontaneous activity.

Best frequency and threshold distributions

BFs of cells from young adult and aged animals ranged from ~2 to 12 kHz (the upper frequency limit was induced by our sound system and does not reflect the upper limit of audible frequencies for gerbils). Neurons with BFs >6 kHz seemed slightly overrepresented in the population of neurons from aged animals. However, the difference in median of both populations was not statistically significant (supplemental Fig. 1A, available at www.jneurosci.org as supplemental material) (Wilcoxon's rank sum test, $p = 0.1$).

Single-neuron thresholds were significantly elevated in the population of older compared with younger animals (supplemental Fig. 1B, available at www.jneurosci.org as supplemental material) (median young adult, 53 dB SPL; median aged, 64 dB SPL; $p = 1 \times 10^{-5}$, Wilcoxon's rank sum test). To test whether, as a consequence, frequency tuning was severely altered, we measured the width of frequency tuning functions 10 dB above threshold ($Q_{10\ dB}$). We found $Q_{10\ dB}$ values not to differ significantly between young adult and aged animals (Wilcoxon's rank sum test, $p = 0.2$), allowing for the following direct comparison of the neuronal responses.

Temporal response patterns and spontaneous activity

Spontaneous activity was measured over 7 s for 89 neurons in young adult and 103 neurons in aged animals. Sixty-one percent (55 of 89) of young adult neurons and 52% (53 of 103) of aged neurons showed spontaneous discharge rates ranging from 0.1 to 40 Hz. Distributions of spontaneous activity did not differ significantly between aged and young adult animals (Wilcoxon's rank sum test, $p = 0.7$).

To obtain a characterization of the distribution of temporal discharge patterns in populations of neurons from young adult and from aged animals, we sorted neurons into eight classes based on response patterns to (1) a 100 ms pure tone at BF 20 dB above pure tone threshold and (2) a 250 ms broadband noise pulse 20 dB above noise threshold. Neurons were clustered based on their onset component (first 50 ms of stimulation), ongoing component (remaining time of stimulation, 50 ms for tones and 200 ms for noise), and offset component (20–150 ms after stimulus offset for tones and 20–500 ms after stimulus offset for noise) (for classification scheme and representative neurons from every class, see Table 1 and Fig. 2). Separate classes were defined for primary-like and sustained neurons that showed spontaneous activity, because the relationship of driven rate to spontaneous activity influenced responses to the pulse matrix (see Fig. 7, sub, plb).

Populations of neurons from both age groups showed similar distribution of temporal discharge patterns in response to pure tones (differences were not statistically significant; bootstrapping, see Material and Methods) (Table 2). In response to stimulation with 250 ms broadband noise pulses, distributions of temporal response patterns differed between populations (Table 2). (1) In response to noise pulses, 10% (9 of 87) of the young adult but only 2% (2 of 94) of the aged population were not or only sparsely driven (Table 2) ($p = 1 \times 10^{-3}$ bootstrapping). (2) The number of primary-like responders with and without spontaneous activity increased from 24% (21 of 87) of young adult to 39% (37 of 94) of aged neurons (Table 2) ($p = 6 \times 10^{-4}$ boot-

Table 2. Distribution of temporal response patterns

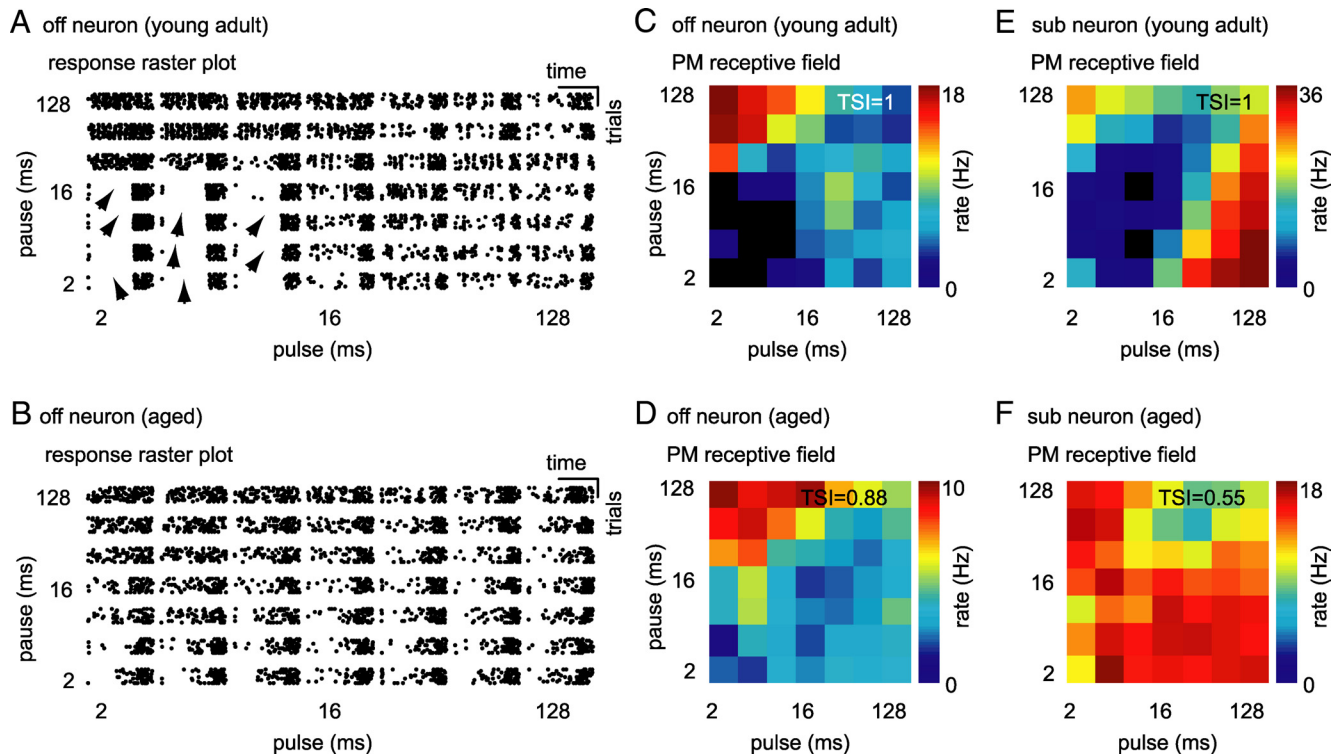|	Sparse	Onset	Primary-like	Sustained	Primary-like spontaneous	Sustained spontaneous	Late sustained	Offset
Tones								
Young (n = 95)	1%	10%	17%	39%	5%	17%	10%	1%
Aged (n = 77)	0%	10%	15%	31%	5%	24%	14%	0%
Noise								
Young (n = 87)	10%	8%	14%	21%	10%	24%	6%	7%
Aged (n = 94)	2%	5%	21%	19%	18%	21%	8%	5%

Figure 3. Single-neuron responses to pulse matrix. **A**, Raster plot of an offset neuron from a young adult animal. This neuron responded preferentially to pulse trains of short pulse and long pause durations; it was not driven by stimuli of short pulse and short pause duration. Stimuli that suppressed response are indicated by arrows. **B**, Raster plot of an offset neuron (off) from an aged animal. This neuron responded preferentially to pulse trains of short pulse and long pause durations, but it was also driven by stimuli of short pulse and pause durations. Discharge of this neuron was not suppressed by any stimulus in our set. **C**, 3-D rate function (PM receptive field) of the offset neuron presented in **A** (young adult). Each square in the surface plot represents the average rate over nine repetitions of the pulse train. Discharge rate is color coded (black, no discharge; dark red, maximum discharge). TSI in the right top corner gives the difference between maximum and minimum discharge rate divided by the maximum discharge rate of the neuron in response to the pulse matrix. **D**, PM receptive field for the offset neuron presented in **B** (aged). **E**, PM receptive field for a sustained spontaneous (sub) neuron from a young adult animal. **F**, PM receptive field for a sustained spontaneous (sub) neuron from an aged animal. Note that discharges of young adult neurons presented in this figure were completely suppressed by a subset of pulse trains from the pulse matrix (TSI = 1), but the discharges of aged neurons were never completely suppressed (TSI = 0.55 and TSI = 0.88).

strapping). There was no obvious relation between the temporal spike pattern of a neuron in response to pure tones and its temporal spike pattern in response to broadband noise.

Most spontaneously active neurons recovered spontaneous activity during the 500 ms silent interval between noise burst repetitions (24 of 29 neurons in young adult animals; 39 of 46 neurons in aged animals). In spontaneously active neurons from young adult animals that recovered spontaneous activity during the 500 ms silent interval between noise burst repetitions, we observed, after stimulus offset, a dip in firing rate that persisted for ~150 ms. The sole exception to this rule were six of the seven offset responders and neurons with very low spontaneous activity (<0.5 Hz). In contrast, in aged animals, beside all offset neurons, eight primary-like neurons discharged within 150 ms after stimulus offset (Fig. 2 *B*,*F*,*G*) with discharge rate >3 Hz. This change in discharge behavior after noise pulses may influence processing

of temporal sequences of information, e.g., the detection of temporal gaps, forward masking, and AM processing.

Neuronal responses to the pulse train stimulation

Next, we evaluated neuronal selectivity to temporal modulations of stimulus amplitude. We recorded from 95 IC neurons from aged and 92 IC neurons from young adult animals, while stimulating the contralateral ear with a matrix of trapezoid noise pulses of varying pulse and pause duration (PM) (see Materials and Methods and Fig. 1). Because there is evidence that the temporal code for AMs in the auditory brainstem is, by and large, converted to a rate code in the IC (Langner and Schreiner, 1988; Langner, 1992; Frisina, 2001; Joris et al., 2004), we focused our analysis on discharge rate.

In Figure 3, we present response patterns (raster plots) and PM receptive fields of two example neurons from young adult
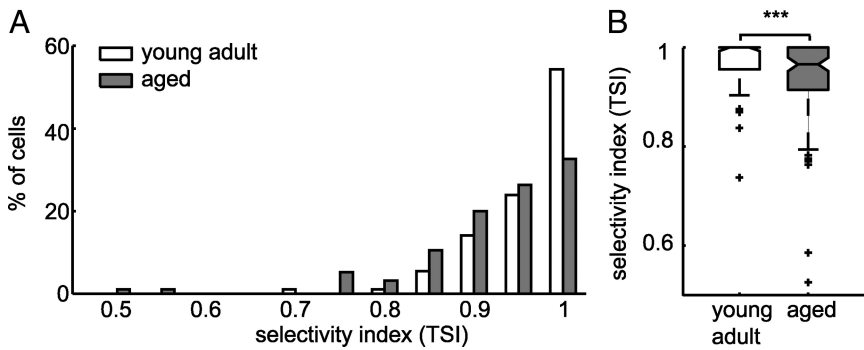
Figure 4. Decrease in temporal selectivity in aged animals. **A**, Distribution of TSIs of neurons from young adult (white) and aged (gray) animals. TSI is the difference between maximum and minimum discharge rate divided by the maximum discharge rate of each neuron in response to the pulse matrix. More neurons from young adult animals did not respond to a subset of pulse trains (TSI = 1), and more neurons from aged animals responded with >6% (TSI < 0.94) of their maximum discharge rate to every pulse train from the pulse matrix. **B**, Box plot of selectivity indices. Temporal selectivity was significantly lower for aged neurons (Wilcoxon's rank sum test, ***$p = 8 \times 10^{-4}$).

(Fig. 3 A,C,E) and two example neurons from aged (Fig. 3 B,D,F) animals. The two neurons shown in Figure 3, A, C (young adult neuron) and B, D (aged neuron), were offset responders. Both neurons were driven to their highest discharge rates by pulse trains composed of long pause and short pulse durations. The neuron from the young adult animal was not (Fig. 3 A,C) but the aged neuron was weakly (Fig. 3 B,D) driven by pulse trains composed of short pulse and short pause durations. In Figure 3, E (young adult) and F (aged), two sustained neurons are presented. Both neurons showed spontaneous activity. However, the cell from the young adult group ceased discharging after sound offset for 0.17 ± 0.02 s and then recovered spontaneous activity, whereas the cell from the aged group did not cease to discharge after sound offset but immediately recovered spontaneous activity. The young adult neuron was driven maximally by pulse trains composed of long pulse and short pause durations or short pulse and long pause durations (Fig. 3 E). This cell did not discharge when stimulated with sounds of short to medium pulses in combination with pauses of medium length. In contrast, the neuron from an aged animal was driven by every single pulse train in our PM. Only small modulations in discharge rate are apparent from the PM receptive field of this neuron (Fig. 3 F). In this set of examples, neurons recorded from young adult animals responded to only a subset of temporal modulations from PM. In contrast, neurons recorded from aged animals responded to every pulse train they were presented with. This suggests that neurons from aged animals might be less selective to pulse–pause combinations than neurons from young adult animals.

Neuronal temporal selectivity to sound pulse and pause duration

To test whether the observed decrease in selectivity to temporal modulations of neurons from aged animals was stable over the population, we (1) compared the relative range of discharge rate modulation (using a temporal selectivity index), and (2) the width of PM receptive fields. The TSI was defined as the difference between the cell-specific maximum in discharge rate evoked by PM to the minimum discharge rate evoked by PM, divided by the maximum discharge rate. The index consequently assumes a value of 1, if the cells discharge rate is modulated to 0 in response to any pulse train in our PM (and the neurons response is therefore highly selective), and assumes a value of 0, if the cells discharge rate is

constant over the PM space (and the neurons response is therefore unselective). The young adult cells displayed in Figure 3, C and E, modulated their discharge to 0 in response to a subset of pulse trains, and their TSIs are therefore 1. In contrast, discharge rates of aged cells shown in Figure 3, D and F, were modulated to at most 22 and 45% of their respective maxima in driven rate, resulting in TSIs of 0.88 and 0.55, respectively.

Indeed, the distribution of selectivity indices for the entire population of neurons from aged animals was significantly shifted toward lower values relative to selectivity indices of neurons from young adult animals (Fig. 4 A,B) (Wilcoxon's rank sum test, $p = 8 \times 10^{-4}$). The observed shift in distributions in aged animals resulted (1) from a decreased number of highly selective cells (31 of 95 neurons in aged vs 50 of 92 neurons in young adult animals with TSI = 1) and (2) from an increase in the number of cells that responded with >6% of their maximum discharge rate to least favorable pulse trains (cells with a TSI <0.94). This difference was evident for cells of all temporal response patterns. However, it was particularly salient for cells that showed primary-like responses while presented with broadband noise and were spontaneously active and for offset neurons.

Although the IC has been under investigation for decades, its functional and computational role is still under debate. It is, however, common knowledge that many IC cells exhibit nonlinearities in their response profiles (e.g., non-monotonic rate level functions, SAM bandpass tuning). The selective suppression of response observed here to a subset of pulse trains represents such a nonlinearity. From now on, we will refer to this nonlinearity as "suppression." In this context, suppression does not necessarily mean suppression as a direct consequence of inhibition but as a consequence of computations at some level that might have involved inhibition.

Having observed a decreased number of highly selective cells in aged animals, we were prompted to ask whether pulse trains that were suppressive to the remaining highly selective cells in aged animals were in their temporal parameters consistent to pulse trains that were suppressive to highly selective cells in young adult animals. To test this, we computed the frequency with which responses to each pulse train were suppressed in the aged and in the young adult population. In neurons from both populations, pulse trains that were composed of long pulses and short pauses were more likely to elicit a response than pulse trains composed of short durations and long pauses (Fig. 5 A,B). However, if we subtracted probability distributions for both populations from each other, it became apparent that long pulse durations (>16 ms) were even less suppressive to aged neurons than to young adult neurons (Fig. 5 C). Pulse trains composed of short durations (<16 ms) and short pauses (<8 ms) were more likely suppressive to young adult compared with aged neurons. Pulse trains composed of short pulses (<16 ms) and long pauses (>4 ms) were more likely to suppress discharges in neurons in aged animals (Wilcoxon's rank sum test, $p = 0.04$). Together, trains of long pulses independent of pause duration and trains of short pulses and short pauses were less likely suppressive to neurons from aged animals than to neurons from young adult animals. Furthermore, although we observed overall fewer neurons

in aged animals that were suppressed by any pulse train from PM, more aged neurons than young adult neurons were suppressed by pulse trains with short pulse and long pause durations. It is interesting to note that, although the set of pulse trains that is more likely suppressive to neurons from young animals comprises pulse trains that, starting from stimulus onset, feed sound energy into the system over a long period of time, the set of pulse trains that is more likely suppressive to neurons from aged animals feeds energy only transiently. The loss of complete suppression in aged animals is therefore highly dependent on the temporal dynamics of the stimulus.

Besides a decrease of highly selective neurons in aged animals, we observed an increase of neurons that responded with a minimum rate to PM that was >6% of the maximum discharge rate to PM. Because TSI measures the relative dynamic range of discharge rates across all pulse trains from PM, it is possible that aged neurons compensate for the loss of selectivity by increasing their maximum discharge rate and thereby maintain their absolute dynamic range of discharge rates. However, we found maximum discharge rates to be invariant but minimum discharge rate to be significantly elevated in aged animals (Wilcoxon's rank sum test, $p = 0.046$). Furthermore, if we considered maximum and minimum discharge rates in relation to TSI, we observed a significant increase of maximum and minimum discharge rates with decreasing TSI in young adult animals (maximum, $r = -0.5$, $p = 5 \times 10^{-7}$; minimum, $r = -0.9$, $p = 1.8 \times 10^{-29}$) (Fig. 6A). For neurons in aged animals, maximum discharge rates were invariant over TSI ($r = 0.05$, $p = 0.6$) (Fig. 6A) and minimum rates increased with decreasing TSI ($r = -0.8$, $p = 1 \times 10^{-22}$) (Fig. 6A). Although we did not observe a change in absolute dynamic range of discharge rate between young adult and aged animals, we observed a significant change in the relation of the absolute dynamic range of discharge rate and TSI: young adult neurons with low TSI modulated their discharge rate over a larger absolute dynamic range in response to PM than aged neurons with low TSI (Fig. 6B).

The observation that minimum discharge rate to PM increased but maximum discharge rate was invariant in aged relative to young adult animals and that cells with low TSI modulated their discharge rate over a smaller absolute dynamic range in response to PM suggests that PM receptive fields are less sharply tuned in aged than in young adult animals. Response rate functions to amplitude modulations are classically analyzed using a threshold criterion (Langner and Schreiner, 1988). Type and width of receptive fields for each neuron are then defined based on AM parameters that elicit a discharge rate that exceeds the
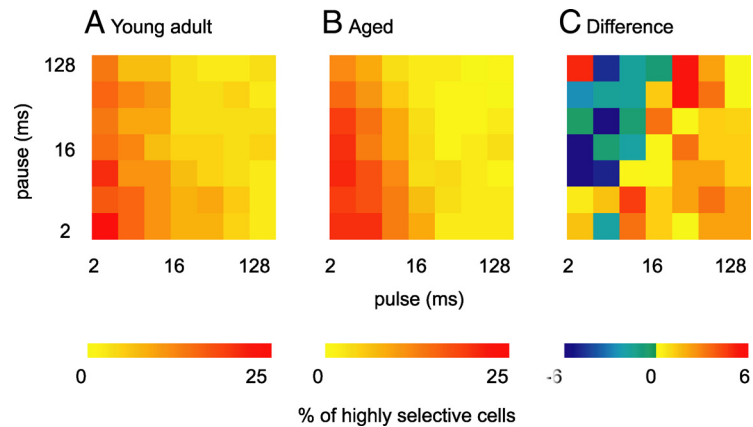

Figure 5. Suppressive effect of pulse trains on neurons from young adult and aged animals. **A**, Probability of each pulse train from the pulse matrix to suppress neurons from young adult animals. Each square in the surface plot depicts the percentage of cells the pulse train of the indicated pulse and pause duration was suppressive to. Percentage is color coded. Discharges of neurons from young adult animals were mostly suppressed by pulse trains of short pulse and short pause durations. **B**, Probability of each pulse train from the pulse matrix to suppress neurons from aged animals. Similar to young adult animals, discharges of neurons from aged animals were most effectively suppressed by pulse trains of short pulse and short pause durations **C**, Difference between probability distributions of pulse trains suppressing neurons from young adult and from aged animals, respectively. Pulse trains of long pulse durations independent of pause duration and pulse trains of short pulse and pause duration were more likely to suppress discharges in young adult animals than in aged animals. Pulse trains of short pulse duration and long pause duration were more likely to suppress discharges in aged animals (Wilcoxon's rank sum test, $p = 0.04$).
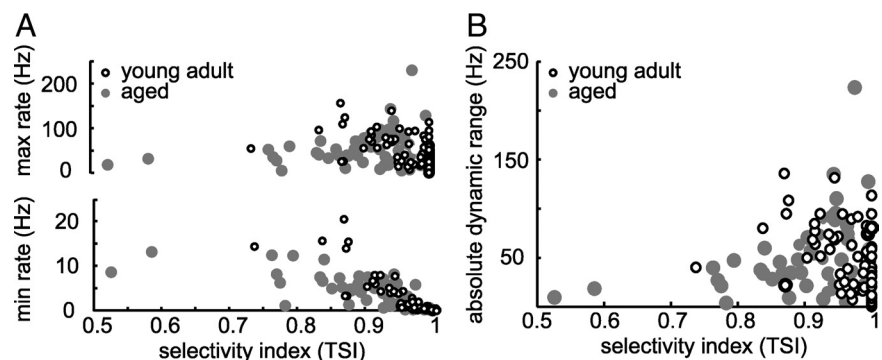

Figure 6. Decreased dynamic range of discharge to pulse matrix in aged neurons with low selectivity indices. **A**, Maximum (top) and minimum (bottom) discharge rates in response to PM in relation to the TSI. Maximum and minimum discharge rates in response to PM increased with decreasing TSI for neurons from young adult animals (maximum, $r = -0.5$, $p = 5 \times 10^{-7}$; minimum, $r = -0.9$, $p = 1.8 \times 10^{-29}$), but maximum discharge rate remained constant and minimum discharge rate increased with decreasing TSI in aged animals (maximum, $r = 0.05$, $p = 0.6$; minimum, $r = -0.8$, $p = 1 \times 10^{-22}$). **B**, Absolute dynamic range of discharge rate in response to PM for neurons from young adult (white) and neurons from aged (gray) animals. Neurons with low TSI from aged animals showed smaller dynamic ranges than neurons with low TSI from young adult animals (correlation between TSI and absolute dynamic range for young adult animals, $r = -0.43$, $p = 2 \times 10^{-5}$; for aged animals, $r = 0.03$, $p = 0.7$).

chosen threshold. If we chose a threshold criterion of up to 10%, we observed a significant increase in receptive field width in the population from aged animals relative to the young adult population (Wilcoxon's rank sum test, $p = 0.04$). As for the suppressive pulse trains, we asked whether pulse trains that elicited a discharge that exceeded threshold were comparable for both populations. For each response type, we calculated the probability that a certain pulse train would drive a cell from this group to a discharge that exceeded threshold. As can be inferred from the resulting 2-D histograms (Fig. 7), tuning is primarily consistent within response types (dark red areas). Neurons from aged and from young adult animals shared preferences for similar pulse trains. However, because the relative range of discharge rates was compressed in aged animals, neurons from all response types
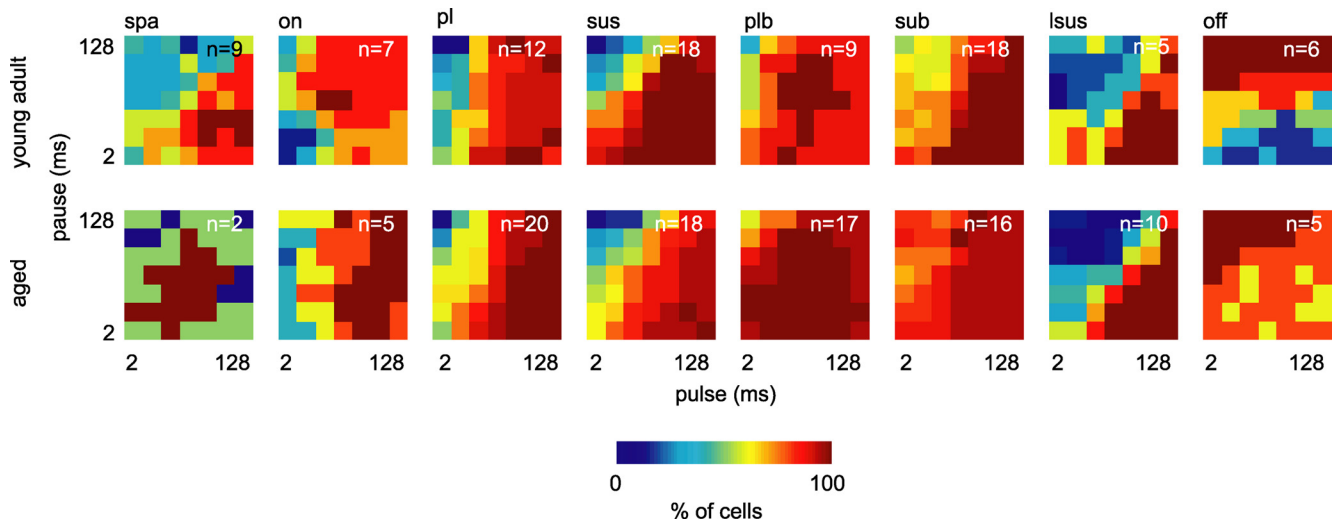
Figure 7. Increased width of PM receptive fields in aged animals. Neurons were grouped according to neuronal response type. Surface plots of 2-D histograms summarize numbers of neurons of each response type that responded with a rate >10% of their maximum discharge to the indicated pulse trains. The top shows neurons from young adult, and the bottom shows neurons from aged animals. Dark blue signifies that the corresponding pulse train was very unlikely to elicit a response >10% of maximum discharge and dark red that the corresponding pulse train elicited a response >10% of maximum discharge in all neurons tested. Note that dark red areas are particularly large for primary-like spontaneous (plb), sustained spontaneous (sub), and offset neurons from aged animals. Over all neurons recorded, the number of pulse trains per neuron that elicit a discharge rate >10% of the maximum discharge rate was significantly higher in aged animals (Wilcoxon's rank sum test, $p = 0.04$). spa, Sparse; on, onset; sus, sustained; pl, primary-like spontaneous; sub, sustained spontaneous; plb, primary-like spontaneous; lsus, late sustained/build-up; off, offset/inhibitory.

showed less selectivity to PM. It is important to note that we did not subtract spontaneous activity for this measure of selectivity. Subtracting spontaneous activity would mask the effect of the decrease in pulse train selectivity, because effects of pulse train stimulation on spontaneous activity differ between young adult and aged animals. Although 30% of neurons from the young adult population significantly suppressed below spontaneous activity (14 of 48 neurons suppressed overall 346 of 2352 pulse trains below spontaneous activity), only 10% of neurons from aged animals suppressed significantly below spontaneous activity (8 of 87 neurons suppressed 128 of 4214 pulse trains below spontaneous activity) in response to pulse train stimulation. Moreover, young adult neurons suppress responses to significantly lower discharge rates below spontaneous activity (Wilcoxon's rank sum test, $p = 2 \times 10^{-6}$). The increase in receptive field width was particularly pronounced for primary-like and sustained neurons that showed spontaneous activity (Fig. 7, plb, sub). From the group of spontaneously active neurons, neurons that discharged shortly (within 150 ms) after stimulus offset (Fig. 2B,G) had particularly wide receptive fields (for five of seven neurons, discharge rate in response to every pulse train from PM exceeded threshold).

Preference in discharge for sound pulse and pause duration
In the preceding paragraphs, we have shown that neurons from aged animals hardly modulate their responses significantly below spontaneous activity and that the number and the pattern of pulse trains that are suppressive to IC neurons changes. These changes in temporal processing not only imply a decrease in temporal selectivity but also a change in preference for temporal parameters (which corresponds to a change in shape of receptive fields) in neurons from aged animals. To test whether receptive field shape was altered in aged relative to young adult animals, we performed PCA on both PM receptive field populations. PCA performs linear transformations on multidimensional data, thereby generating a new set of variables, called principal components (PCs). Because all the PCs are orthogonal to each other

(there is no redundant information), the set of PCs explains the variance in the data ideally with fewer variables than the original data. When analyzing PM receptive fields of neurons from young adult and aged animals separately, we found that, for sustained neurons from aged animals, 90% of the variance was explained by the first and only 10% by the second PC (Fig. 8A). In contrast, for sustained neurons from young adult animals, 50% of the variance of PM receptive fields was explained by the first, 30% by the second, and 10% by the third PC (Fig. 8A). The difference in variance explained indicates that PM receptive fields of sustained neurons from young adult animals may be more variable in shape than those from aged animals. To test this, we performed PCA on the joint population of PM receptive fields from young adult and aged animals. As for young adult and aged animals separately, for the joint population of PM receptive fields, the most influential component represented a shift in discharge rate for long pulse and short pause durations, the second PC represented a scaling of the preference for pulse trains of short pulse and short pause durations, and the third PC represented a shift toward short to medium pulse and long pause durations (Fig. 8B, left). The representation of the original PM receptive fields in principal component space is reflected in the neuron-specific weights for each PC. As expected, weights for PC 3 were significantly more variable in young adult than in aged animals (Fig. 8B, right) (Ansari-Bradley test, $p = 0.02$). To understand the influence of PCs 1–3 on individual PM receptive fields, we sorted neurons into clusters based on their representations in PC space (see Materials and Methods). Neurons formed three robust clusters: the mean distance of each neuron to the centroid of its assigned cluster (0.04 ± 0.007) was two orders of magnitude smaller than the mean distance between centroids of different clusters (1.4 ± 0.4), and cluster centroids were significantly different (MANOVA, $p = 1 \times 10^{-7}$). The first cluster consisted of neurons showing a preference for short pulse and short pause durations and in addition a duty cycle preference (Fig. 8C, top left). The second cluster consisted of neurons showing a strong duty cycle preference (Fig. 8C, top right). This cluster was mostly dominated by
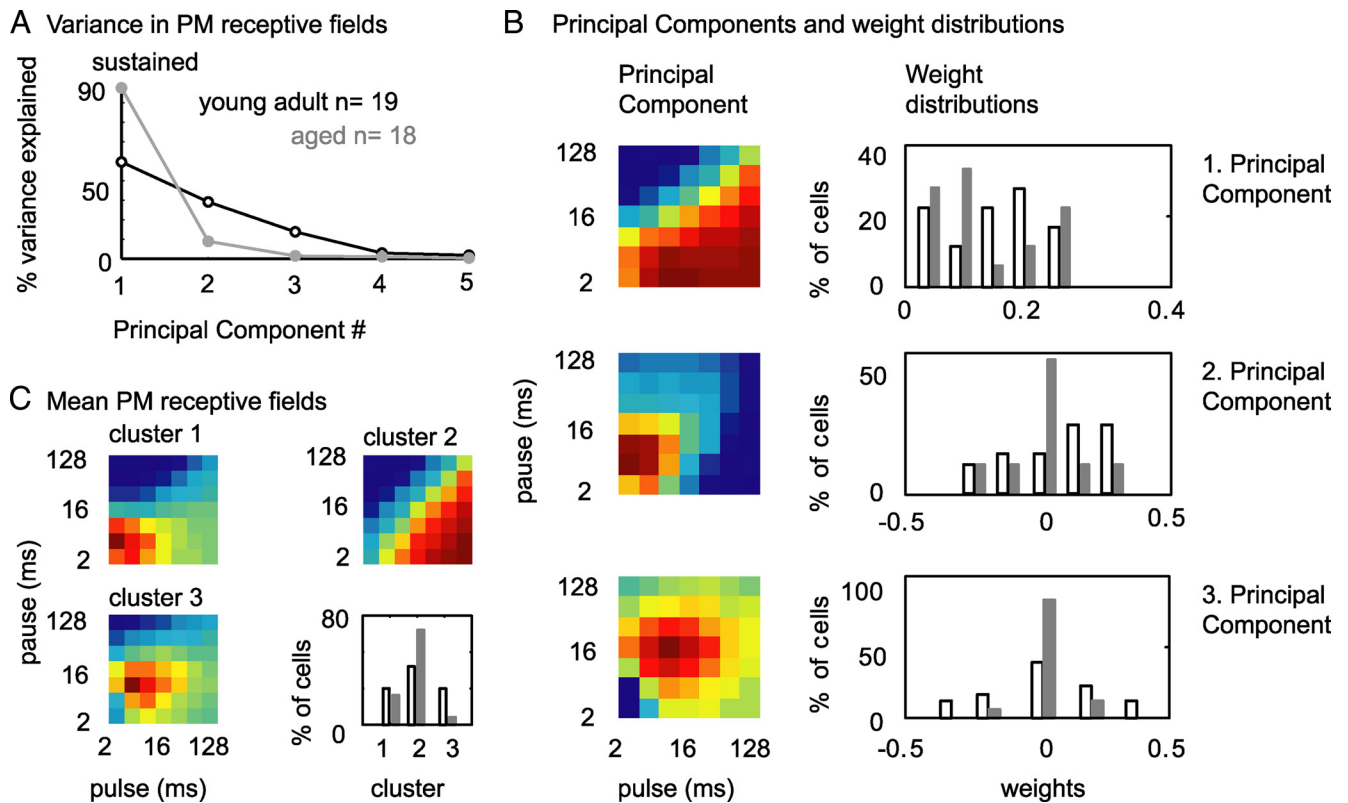
A Variance in PM receptive fields

B Principal Components and weight distributions

C Mean PM receptive fields

Figure 8. Strong duty cycle preference in PM receptive fields of sustained neurons from aged animals. *A*, Variance in PM receptive fields of sustained neurons from young adult and aged animals explained by PCs. PCs were computed from PM receptive fields of young adult and aged animals separately. For sustained neurons from young adult animals, 50% of the variance is explained by the first, 30% by the second, and ∼10% by the third PC. In contrast, in the aged population, 90% of the variance is explained by the first and only 10% by the second PC. *B*, First, second, and third PC of PM receptive fields of sustained neurons from young adult and aged animals. In all the 3-D plots, dark red depicts strong responses and dark blue weak responses. Distributions of weights for principal components of individual PM receptive fields are shown in the right. Weights for the second PC tend to more positive values for young adult than for aged animals (not significant). Weights for the third PC tend to cluster around 0 for aged but are spread to positive and negative values for young adult animals (Ansari-Bradley test, $p = 0.02$). *C*, Mean PM receptive fields of neurons from young adult and aged animals. Neurons were clustered based on their representation in three-dimensional principal component space (weights). Note that cluster 2 comprises neurons that showed a strong preference in discharge for short duty cycles and was mostly dominated by neurons from aged animals. Cluster 3 comprised neurons that showed a clear preference for pulse trains with short to medium pulse and pause durations. This cluster was dominated by sustained neurons from young adult animals.

neurons from aged animals (13 of 18 neurons from aged and 8 of 19 neurons from young adult animals). The third cluster consisted of neurons showing a strong preference for short pulse and short pause durations (Fig. 8*C*, bottom left). This cluster was clearly dominated by neurons from young adult animals (5 of 19 neurons from young adult and 1 of 18 neurons from aged animals). Together, a clear preference for short pulse and pause durations seemed to be lost in sustained neurons from aged animals. Instead, 72% of neurons showed wide receptive fields with a preference for pulse trains with short duty cycles. This corresponds to a change in shape of PM receptive fields in favor of pulse trains with long pulse and short pause durations and therefore an unselective response for a sustained neuron.

Neurons from other response type classes did not show significant changes in PM receptive field variety when analyzed with PCA.

Similarity of temporal receptive fields
Over the populations of IC neurons from young adult and aged animals, a decrease in temporal selectivity and a decrease in variety of shape of temporal receptive fields should amount to an increase in similarity of temporal receptive fields within the population of IC neurons from aged animals. To quantitatively analyze the similarity of PM receptive fields, we correlated PM receptive fields of every possible pair of cells within both popula-

tions. If PM receptive fields of a pair of neurons congruently vary with temporal parameters, correlation of this pair of neurons will be strong and positive (correlation at ∼1); if, conversely, PM receptive fields of a pair of neurons vary opposite to each other, correlation of this pair of neurons will be strong and negative (correlation at approximately −1). In Figure 9*A*, we present a pair of neurons from young adult animals (*A*, left, lsus; *A*, right, off) whose PM receptive fields run nearly opposite to each other ($r = -0.76$). Distributions of pairwise correlation coefficients (*r*) of all neurons from young adult and from aged animals are plotted in Figure 9*B*. Compared with the distribution of *r* of pairs of neurons from young adult animals, the distribution of *r* of neurons from aged animals shows a trend to more positive values. In particular, strong and medium negative correlations are diminished and weak and strong positive correlations are increased across the aged population of cells (Wilcoxon's rank sum test, $p = 9 \times 10^{-8}$). This indicates an increased similarity of the responses of aged neurons to PM.

Together, we observed an increase in signal correlations (and therefore in similarity) in response to PM in our sample of neurons from aged animals. This increase in signal correlations was attributable to a reduced number of sparse responders and an increased similarity of PM receptive fields in terms of PM receptive field shape and width of sustained responders, primary-like responders, and off responders both within and across response
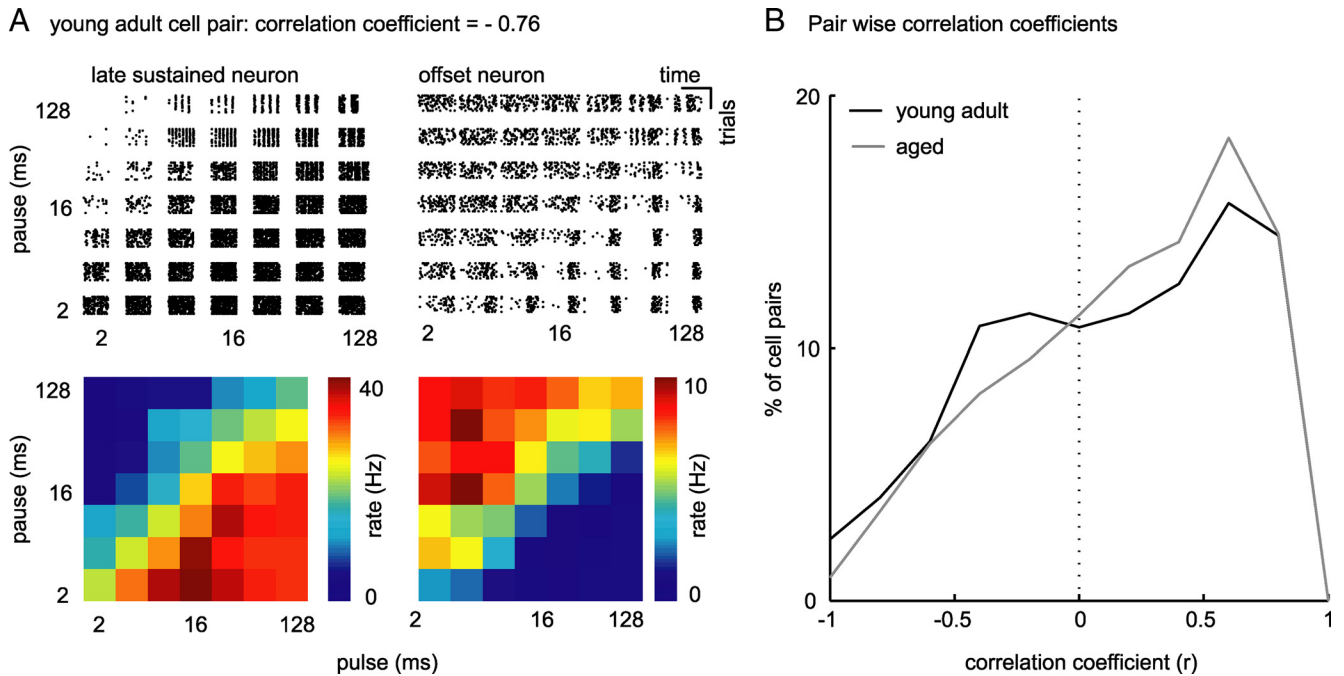
Figure 9. Increase in strong positive correlations between pairs of neurons from aged animals. **A**, Raster plots and PM receptive fields of two example neurons from a young adult animal. Neuronal response types were late sustained (left) and offset (right). The sustained neuron was well driven by pulse trains of long pulse and short pause durations, whereas the offset neuron was hardly driven by these stimuli. Receptive fields of these two neurons were therefore of nearly opposite directions (correlation coefficient, $r = -0.76$). **B**, Probability distribution of r of all possible pairs of neurons from young adult (black) and aged (gray) animals. Significantly less pairs of neurons from aged animals show high negative correlations (Wilcoxon's rank sum test, $p = 1.8 \times 10^{-4}$).

types. The population of aged neurons was, in other words, less heterogeneous in its preference for temporal modulations than the sample of young adult neurons.

Encoding of speech
The temporal parameters that varied across pulse trains in the PM were pulse and pause duration. Pulse and pause duration, along with rise–fall times and the dependent parameters, duty cycle and modulation frequency, define amplitude modulations of natural communication signals. We assume that, if receptive fields for sound pulse and pause duration are less heterogeneous across neurons from aged animals, this set of neurons will be less efficient in representing complex natural AM signals occurring in speech. To test this, we presented young adult and aged animals with eight different German speech snippets taken from a clinical test (Oldenburger Satztest; courtesy of Dr. Birger Kollmeier) while recording single-unit responses from 57 neurons from young adult and 47 neurons from aged animals. From neural responses to these sentences, we cut the first 125 ms for analysis (Fig. 10A). We quantified how well speech snippets can be separated based on rate responses of single neurons. To achieve this, we decoded the set of speech snippets in terms of dissimilarity of rate responses. To decode a response evoked by one trial of one speech snippet from our set, we removed the response from the set and used a distance metric to infer the stimulus that evoked it. We then choose the stimulus corresponding to the response to which the distance to the response we picked was minimal. To decode speech snippets from populations of neurons, we calculated distances for each cell separately and then summed distances over cells before decoding. We found that our set of eight speech snippets was decoded equally well from single-neuron responses from young adult and aged animals (distributions of percentage correct did not differ significantly between young adult and aged animals, $p = 0.9$). Based on our observation that

neurons from aged animals were less selective to temporally modulated sounds and therefore heterogeneity of responses was reduced, we hypothesized that, although single neurons from aged animals encoded this set of eight speech snippets reliably, joint encoding was less beneficial for aged than for young adult animals. To test this, we computed (1) for each neuron, the percentage correct classification of speech snippets based on the single neuron response and, (2) for each possible pair of neurons (within each population), the percentage correct classification based on paired single-neuron responses (Fig. 10B). We then measured the increase in percentage correct classification of speech snippets (benefit) based on the paired response, relative to the percentage correct classification of speech snippets based on separate responses (Fig. 10B, arrows). When we compared benefits of joint encoding across populations, it became apparent that, for young adult animals, the benefit of taking a second cell into account was significantly greater than for aged animals (Wilcoxon's rank sum test, $p = 7 \times 10^{-13}$) (Fig. 10C). This indicates that, although rate responses of neurons from aged animals to this set of speech snippets were still dissimilar enough to decode the speech snippets correctly, neurons from aged animals responded to more similar temporal features, which significantly decreased the benefit of joint encoding based on discharge rate.

Discussion
We searched for a neural correlate of the psychophysically, for humans (Strouse et al., 1998) and gerbils (Hamann et al., 2004), reported deterioration of temporal processing in the aged auditory system. Our results provide evidence that the representation of temporal parameters is significantly altered in the IC of aged gerbils. IC neurons in aged animals show significantly reduced selectivity and variety in tuning to the duration of sound pulses and pauses. The reduction in selectivity and variety leads on the population level to a decrease in heterogeneity of temporal recep-
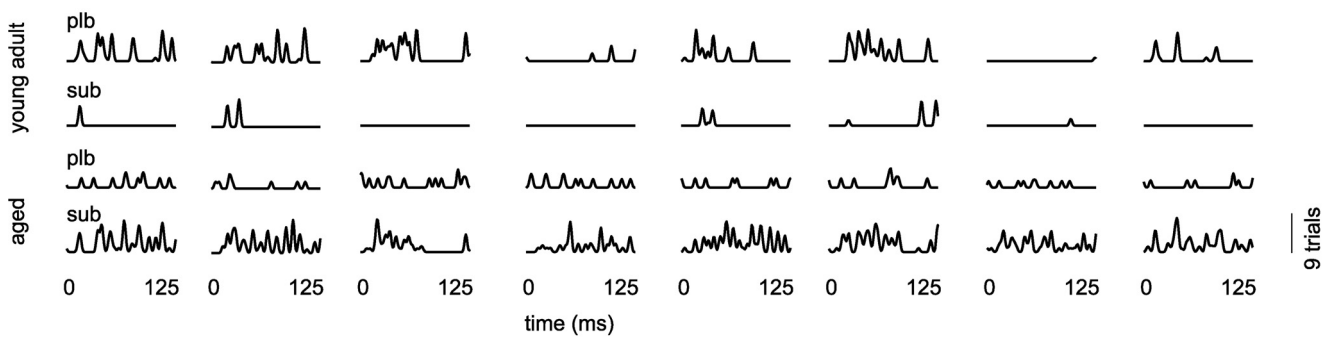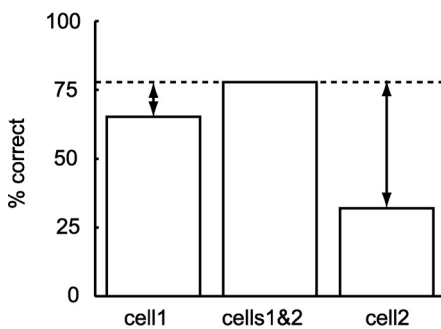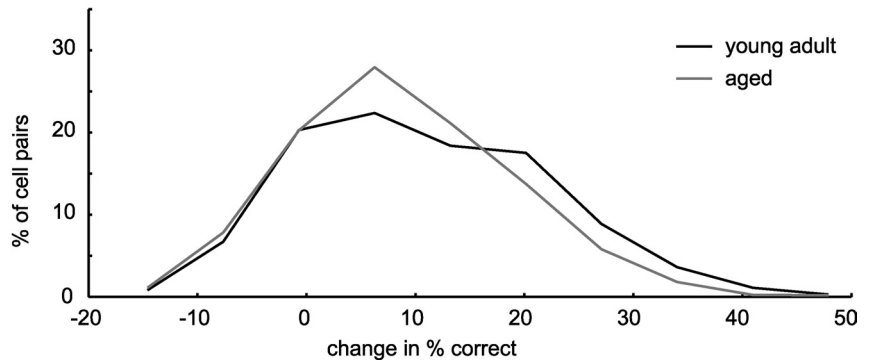
A Smoothed PSTHs of single neuron responses

B Benefit of paired encoding

C Distribution of benefit of paired encoding

Figure 10. Decrease in benefit of joined encoding of speech for pairs of neurons from aged animals. ***A***, Smoothed PSTHs of neuronal responses to 125 ms speech snippets from one primary-like spontaneous (plb) and one sustained spontaneous (sub) neuron from a young adult animal (top 2 rows) and from an aged animal (bottom 2 rows), respectively. ***B***, Neuronal responses to eight speech snippets were decoded based on dissimilarity of rate responses using a distance metric. Benefit of pairwise encoding was defined as the difference between classification success of every possible pair of neuron (cells1&2) and each neuron separately (cell1, cell2). Arrows indicate benefit of paired encoding. ***C***, Probability distribution of benefit of paired encoding for neurons from young adult (black) and aged (gray) animals. Benefit of paired encoding was significantly larger for neurons from young adult than for neurons from aged animals (Wilcoxon's rank sum test, $p = 7 \times 10^{-13}$).

tive fields and results in inefficient encoding of natural stimuli. This is, to our knowledge, the first electrophysiological evidence of an age-related decline in neuronal temporal selectivity and in population coding efficiency in response to complex natural sounds.

Technical considerations

Because we compared responses of neurons from aged animals to neurons from young adult animals, it is important to ensure that we recorded from comparable populations of neurons in both age groups. In our experiments, we used an array of seven electrodes, allowing us to sample the mediolateral and rostrocaudal extent of the IC during each experiment. Moreover, we recorded from neurons with similar distribution of BFs and temporal patterns in response to pure tones in both populations. Given the assumption that certain temporal response patterns cluster in certain areas of the IC, that we limited the range of neurons BF to increase the number of neurons sampled per frequency band, it is unlikely that the differences in response properties we observe are caused by a sampling bias rather than by age-related alterations in neural processing.

Because we find median of pure tone thresholds to be increased but width of frequency tuning at 10 dB above threshold unchanged, there may be, in addition to alterations in central auditory processing also a conductive component to age-related changes of sound processing.

Relation to previous studies

Our results are consistent with previous observation in rats (Shaddock Palombi et al., 2001), mice (Walton et al., 2002), and gerbils (Boettcher et al., 1996). Boettcher et al. (1996) used auditory brainstem recordings to show altered neural processing of short temporal gaps between two successive noise bursts in aged gerbils. Walton et al. (2002) observed that spike rates at best modulation frequencies of SAM stimuli were more variable in young adult than in the aged population of neurons. Shaddock Palombi et al. (2001) observed a decrease in SAM-bandpass-tuned and an increase in SAM-low-pass-tuned neurons in aged animals.

Implications for population coding

One might argue that a decrease in heterogeneity of the neural population creates an overrepresentation of the stimulus and therefore helps to overcome stochastic responses of individual neurons. Conversely, it has been shown that overlapping representation of stimulus features hampers stimulus discrimination (Nadal and Parga, 1994). Depending on the desired outcome, different encoding strategies might therefore be used at different levels of the brain. It has been hypothesized that sensory systems move from redundant encoding in the periphery to an efficient, heterogeneous encoding in higher-level processes (Atick, 1992). Evidence for this organization comes from other sensory modalities, e.g., taste (Rolls and Treves, 1990) and vision (Rolls and Tovee, 1995). For the auditory system, Holmstrom et al. (2010)

reported heterogeneous receptive fields at the level of the IC and hypothesized that the IC plays a critical role in the efficient encoding of auditory information by facilitating the discrimination of behaviorally relevant sounds (Boettcher et al., 1996). Across the population of IC neurons, sound discrimination is facilitated by installing complex selectivity, thereby increasing heterogeneity. Our results show that temporal receptive fields of IC neurons from aged animals are less heterogeneous than temporal receptive fields of IC neurons from young adult animals and encoding of a set of natural stimuli is less efficient in the aged population of neurons. We speculate that, if a more complex set of stimuli was used, responses of single neurons would be less informative and joint encoding would be more important.

Implications for temporal processing

An interesting response property of auditory neurons that can be observed at various levels of the auditory pathway, but is particularly versatile in the IC, is selectivity in discharge rate to temporal features of sound, such as, e.g., amplitude modulations and frequency modulations (Brand et al., 2000; McAlpine, 2004; Woolley and Casseday, 2005; Pérez-González et al., 2006; Krebs et al., 2008). These versatile tuning patterns result from the complex set of synaptic inputs IC cells receive and are therefore dependent on outputs of the various auditory nuclei converging at the IC. The dependence of AM selectivity of single IC neurons on network states is nicely illustrated by the finding that AM selectivity can be modulated by changing sound location (Koch and Grothe, 2000) or by blocking inhibition (Casseday et al., 1994; Fuzessery and Hall, 1996; Casseday et al., 2002). We observed a significant decrease in temporal selectivity of IC neurons in aged animals. As mentioned above, selectivity of IC neurons to temporal features of sound depends critically on a balanced interplay of excitation and inhibition. In line with our results, a severe downregulation of the inhibitory transmitter system has been reported for the aged auditory system (Banay-Schwartz et al., 1989; Milbrandt et al., 1994, 1996, 2000; Willott et al., 1997). Studies of monkey primary visual cortex showed, in accordance with our results, a decreased orientation and direction selectivity of single neurons and orientation selectivity of single neurons to be reinstalled by GABA application (Schmolesky et al., 2000; Leventhal et al., 2003). Similarly, behavioral gap detection thresholds of aged gerbils matched gap detection thresholds of young adult gerbils, when γ-vinyl-GABA was systemically applied (Gleich et al., 2003). Therefore, the decrease in auditory temporal tuning we observed in aged animals may be correlated with the reported downregulation of the inhibitory transmitter systems. If we compare responses of aged neurons from the present study with responses recorded from young adult neurons during blockade of GABA (Faingold et al., 1991; Vater et al., 1992; Caspary et al., 2002) or glycine (Vater et al., 1992), neural response properties are ambivalent. Besides alterations in temporal tuning, increases in evoked and spontaneous rate are commonly observed as a consequence of blocking inhibition in the IC. Consistently with Shaddock Palombi et al. (2001), we did not observe an increase in evoked discharge rate. Indeed, Walton et al. (2002) observed an increase in evoked discharge in aged animals; however, this might be the result of stimulation with higher SPL (Walton et al., 2002). We also did not observe an increase in spontaneous activity in IC of aged gerbil. Spontaneous activity in mouse IC also did not increase with age (Walton et al., 2002). Studies from primary visual (Schmolesky et al., 2000) and auditory (Hughes et al., 2010) cortices report an upregulation of spontaneous activity. If we consider that reports on changes in spontaneous activity are consistent within and differ across brain structures, in the context of a downregulation of the inhibitory neurotransmitter system, it seems reasonable to speculate that different levels of spontaneous activity at different levels of the brain result from homeostatic processes in the neural network that are caused by the imbalance of excitation and inhibition. If we further consider (1) that a severe downregulation of the inhibitory neurotransmitter system has been reported for the entire auditory system and (2) that the IC receives convergent input from almost all other auditory nuclei, it is unlikely that consequences of a decreased weight of inhibitory synapses in the entire auditory system correspond to the consequences of a blockade of inhibition that is confined to an area in the IC. The notion that response properties of IC neurons are not independent but highly dependent on calculations in other nuclei of the auditory system is supported by the findings that (1) only a subset of SAM-tuned IC neurons change their tuning properties after application of GABA (Caspary et al., 2002) and (2) temporal tuning to SAM of IC neurons is inherited from lower brainstem nuclei (Grothe, 1994; Burger and Pollak, 1998; Kuwada and Batra, 1999). In addition, alterations in the transmitter systems might not be exclusive to inhibitory transmitter systems but might also affect the excitatory transmitter systems. A disruption of both excitatory and inhibitory transmitter systems would equally result in an imbalance of synaptic inputs, which would disrupt the computational arrangements in the network.

Together, we showed that synthetic temporal modulations are represented less heterogeneously across the neuronal population and that encoding of natural temporal modulations is less efficient in population of neurons from aged animals. We hypothesize that this deficit may be detrimental for encoding complex sets of temporally modulated signals. We assume that the changes we observe result from alterations in neurotransmitter system that disrupt the computational arrangements in the neural network.

References

Andoni S, Li N, Pollak GD (2007) Spectrotemporal receptive fields in the inferior colliculus revealing selectivity for spectral motion in conspecific vocalisations. J Neurosci 27:4882–4893.

Aronov D (2003) Fast algorithm for the metric-space analysis of simultaneous responses of multiple single neurons. J Neurosci Methods 124:175–179.

Atick JJ (1992) Could information theory provide an ecological theory of sensory processing? Network 3:213–251.

Banay-Schwartz M, Lajtha A, Palkovits M (1989) Changes with aging in the levels of amino acids in rat CNS structural elements. I. Glutamate and related amino acids. Neurochem Res 14:555–562.

Barsz K, Ison JR, Snell KB, Walton JP (2002) Behavioral and neural measures of auditory temporal acuity in aging humans and mice. Neurobiol Aging 23:565–578.

Boettcher FA, Mills JH, Swerdloff JL, Holley BL (1996) Auditory evoked potentials in aged gerbils: responses elicited by noises separated by a silent gap. Hear Res 102:167–178.

Brand A, Urban R, Grothe B (2000) Duration tuning in the mouse auditory midbrain. J Neurophysiol 84:1790–1799.

Brand A, Behrend O, Marquardt T, McAlpine D, Grothe B (2002) Precise inhibition is essential for microsecond interaural time difference coding. Nature 417:543–547.

Burger RM, Pollak GD (1998) Analysis of the role of inhibition in shaping responses to sinusoidally amplitude-modulated signals in the inferior colliculus. J Neurophysiol 80:1686–1701.

Burianova J, Ouda L, Profant O, Syka J (2009) Age-related changes in GAD levels in the central auditory system of the rat. Exp Gerontol 44:161–169.

Caspary DM, Palombi PS, Hughes LF (2002) GABAergic inputs shape responses to amplitude modulated stimuli in the inferior colliculus. Hear Res 168:163–173.

Casseday JH, Ehrlich D, Covey E (1994) Neural tuning for sound duration: role of inhibitory mechanisms in the inferior colliculus. Science 264:847–850.

Casseday JH, Fremouw T, Covey E (2002) The inferior colliculus: a hub for the central auditory system. In: Integrative functions in the mammalian auditory pathway (Oertel D, Popper AN, Fay RR, eds), pp 238–318. New York: Springer.

Chelaru MI, Dragoi V (2008) Efficient coding in heterogeneous neuronal populations. Proc Natl Acad Sci U S A 105:16344–16349.

Ehrlich D, Casseday JH, Covey E (1997) Neural tuning to sound duration in the inferior colliculus of the big brown bat, Eptesicus fuscus. J Neurophysiol 77:2360–2372.

Faingold CL, Boersma Anderson CA, Caspary DM (1991) Involvement of GABA in acoustically-evoked inhibition in inferior colliculus neurons. Hear Res 52:201–216.

Frisina RD (2001) Subcortical neural coding mechanisms for auditory temporal processing. Hear Res 158:1–27.

Fuzessery ZM, Hall JC (1996) Role of GABA in shaping frequency tuning and creating FM sweep selectivity in the inferior colliculus. J Neurophysiol 76:1059–1073.

Gleich O, Hamann I, Klump GM, Kittel M, Strutz J (2003) Boosting GABA improves impaired auditory temporal resolution in the gerbil. Neuroreport 14:1877–1880.

Gordon-Salant S, Fitzgibbons PJ (1993) Temporal factors and speech recognition performance in young and elderly listeners. J Speech Hear Res 36:1276–1285.

Grothe B (1994) Interaction of excitation and inhibition in processing of pure tone and amplitude-modulated stimuli in the medial superior olive of the mustached bat. J Neurophysiol 71:706–721.

Grothe B, Covey E, Casseday JH (2001) Medial superior olive of the big brown bat: neuronal responses to pure tones, amplitude modulations, and pulse trains. J Neurophysiol 86:2219–2230.

Gustafsson HA, Arlinger SD (1994) Masking of speech by amplitude-modulated noise. J Acoust Soc Am 95:518–529.

Hamann I, Gleich O, Klump GM, Kittel MC, Strutz J (2004) Age-dependent changes of gap detection in the Mongolian gerbil (Meriones unguiculatus). J Assoc Res Otolaryngol 5:49–57.

Holmstrom LA, Eeuwes LB, Roberts PD, Portfors CV (2010) Efficient encoding of vocalisations in the auditory midbrain. J Neurosci 30:802–819.

Hughes LF, Turner JG, Parrish JL, Caspary DM (2010) Processing of broadband stimuli across A1 layers in young and aged rats. Hear Res 264:79–85.

Irvine DR, Gago G (1990) Binaural interaction in high-frequency neurons in inferior colliculus of the cat: effects of variations in sound pressure level on sensitivity to interaural intensity differences. J Neurophysiol 63:570–591.

Joris PX, Schreiner CE, Rees A (2004) Neural processing of amplitude-modulated sounds. Physiol Rev 84:541–577.

Koch U, Grothe B (2000) Interdependence of spatial and temporal coding in the auditory midbrain. J Neurophysiol 83:2300–2314.

Krebs B, Lesica NA, Grothe B (2008) The representation of amplitude modulations in the mammalian auditory midbrain. J Neurophysiol 100:1602–1609.

Krenning J, Hughes LF, Caspary DM, Helfert RH (1998) Age-related glycine receptor subunit changes in the cochlear nucleus of Fischer-344 rats. Laryngoscope 108:26–31.

Krishna BS, Semple MN (2000) Auditory temporal processing: responses to sinusoidally amplitude-modulated tones in the inferior colliculus. J Neurophysiol 84:255–273.

Kuwada S, Batra R (1999) Coding of sound envelopes by inhibitory rebound in neurons of the superior olivary complex in the unanesthetised rabbit. J Neurosci 19:2273–2287.

Langner G (1992) Periodicity coding in the auditory system. Hear Res 60:115–142.

Langner G, Schreiner CE (1988) Periodicity coding in the inferior colliculus of the cat. I. Neuronal mechanisms. J Neurophysiol 60:1799–1822.

LeBeau FE, Malmierca MS, Rees A (2001) Iontophoresis in vivo demonstrates a key role for GABA(A) and glycinergic inhibition in shaping frequency response areas in the inferior colliculus of guinea pig. J Neurosci 21:7303–7312.

Leventhal AG, Wang Y, Pu M, Zhou Y, Ma Y (2003) GABA and its agonists improved visual cortical function in senescent monkeys. Science 300:812–815.

McAlpine D (2004) Neural sensitivity to periodicity in the inferior colliculus: evidence for the role of cochlear distortions. J Neurophysiol 92:1295–1311.

Milbrandt JC, Albin RL, Caspary DM (1994) Age-related decrease in GABAB receptor binding in the Fischer 344 rat inferior colliculus. Neurobiol Aging 15:699–703.

Milbrandt JC, Albin RL, Turgeon SM, Caspary DM (1996) GABAA receptor binding in the aging rat inferior colliculus. Neuroscience 73:449–458.

Milbrandt JC, Hunter C, Caspary DM (1997) Alterations of GABAA receptor subunit mRNA levels in the aging Fischer 344 rat inferior colliculus. J Comp Neurol 379:455–465.

Milbrandt JC, Holder TM, Wilson MC, Salvi RJ, Caspary DM (2000) GAD levels and muscimol binding in rat inferior colliculus following acoustic trauma. Hear Res 147:251–260.

Nadal JP, Parga N (1994) Nonlinear neurons in the low-noise limit: a factorial code maximises information transfer. Network 5:565–581.

Oliver DL, Huerta MF (1992) Inferior and superior colliculi. In: The mammalian auditory system: neuroanatomy (Webster DB, Popper AN, Fay RR, eds), pp 168–221. New York: Springer.

Pecka M, Brand A, Behrend O, Grothe B (2008) Interaural time difference processing in the mammalian medial superior olive: the role of glycinergic inhibition. J Neurosci 28:6914–6925.

Pérez-González D, Malmierca MS, Moore JM, Hernández O, Covey E (2006) Duration selective neurons in the inferior colliculus of the rat: topographic distribution and relation of duration sensitivity to other response properties. J Neurophysiol 95:823–836.

Pollak GD, Klug A, Bauer EE (2003a) Processing and representation of species-specific communication calls in the auditory system of bats. Int Rev Neurobiol 56:83–121.

Pollak GD, Burger RM, Klug A (2003b) Dissecting the circuitry of the auditory system. Trends Neurosci 26:33–39.

Rolls ET, Tovee MJ (1995) Sparseness of the neuronal representation of stimuli in the primate temporal visual cortex. J Neurophysiol 73:713–726.

Rolls ET, Treves A (1990) The relative advantages of sparse versus distributed encoding for associative neuronal networks in the brain. Network 1:407–421.

Ryan A (1976) Hearing sensitivity of the mongolian gerbil, Meriones unguiculatis. J Acoust Soc Am 59:1222–1226.

Schmolesky MT, Wang Y, Pu M, Leventhal AG (2000) Degradation of stimulus selectivity of visual cortical cells in senescent rhesus monkeys. Nat Neurosci 3:384–390.

Schuller G, Radtke-Schuller S, Betz M (1986) A stereotaxic method for small animals using experimentally determined reference profiles. J Neurosci Methods 18:339–350.

Shaddock Palombi P, Backoff PM, Caspary DM (2001) Responses of young and aged rat inferior colliculus neurons to sinusoidally amplitude modulated stimuli. Hear Res 153:174–180.

Shamir M, Sompolinsky H (2006) Implications of neuronal diversity on population coding. Neural Comput 18:1951–1986.

Siveke I, Pecka M, Seidl AH, Baudoux S, Grothe B (2006) Binaural response properties of low-frequency neurons in the gerbil dorsal nucleus of the lateral lemniscus. J Neurophysiol 96:1425–1440.

Snell KB (1997) Age-related changes in temporal gap detection. J Acoust Soc Am 101:2214–2220.

Strouse A, Ashmead DH, Ohde RN, Grantham DW (1998) Temporal processing in the aging auditory system. J Acoust Soc Am 104:2385–2399.

van Rossum MC (2001) A novel spike distance. Neural Comput 13:751–763.

Vater M, Habbicht H, Kössl M, Grothe B (1992) The functional role of GABA and glycine in monaural and binaural processing in the inferior colliculus of horseshoe bats. J Comp Physiol A 171:541–553.

Victor JD, Purpura KP (1996) Nature and precision of temporal coding in visual cortex: a metric-space analysis. J Neurophysiol 76:1310–1326.

Walton JP, Simon H, Frisina RD (2002) Age-related alterations in the neural coding of envelope periodicities. J Neurophysiol 88:565–578.

Willott JF, Milbrandt JC, Bross LS, Caspary DM (1997) Glycine immunoreactivity and receptor binding in the cochlear nucleus of C57BL/6J and CBA/CaJ mice: effects of cochlear impairment and aging. J Comp Neurol 385:405–414.

Woolley SM, Casseday JH (2005) Processing of modulated sounds in the sebra finch auditory midbrain: responses to noise, frequency sweeps, and sinusoidal amplitude modulations. J Neurophysiol 94:1143–1157.